

Complexation of a hydrophobic thiazorylazophenol with Ni^{2+} at sodium dodecylsulfate micellar surface

Atsuyuki Ikeya and Tetsuo Okada *

Department of Chemistry, Tokyo Institute of Technology, Meguro-ku, Tokyo 152-8551, Japan

Received 24 October 2002; accepted 28 April 2003

Abstract

Complexation of thiazorylazododecylphenol (TADP) with Ni^{2+} at the surface of sodium dodecylsulfate (SDS) micelles has been spectrophotometrically studied. Complicated spectral changes are analyzed by a factor and multivariate analysis, which implies the formation of $[\text{TDAP}(\text{OH}^-)\text{Ni}]^0$ as well as a simple 1:1 complex of Ni^{2+} with TDAP at the micellar interface. All of the equilibrium constants required to describe this system are substantially affected by electrolyte concentrations. Coexistent electrolytes vary the surface potential of the micelle, and in turn influence the equilibria taking place on the micellar surface. The electrostatic potential estimated based on the equilibrium shifts is more negative than that calculated according to Poisson–Boltzmann theory, which simply involves electrostatic effects. This disagreement is possibly caused by different aqueous environments around the micelle from bulk solution, which also facilitate the formation of unusual complex such as $[\text{TDAP}(\text{OH}^-)\text{Ni}]^0$.

© 2003 Elsevier Inc. All rights reserved.

Keywords: Complexation at SDS micellar surface; Factor analysis; Electrostatic potential

1. Introduction

Self-assembled systems have received increasing attention in various disciplines of chemistry. Current major interests focus on self-assembled monolayers formed on solid surfaces, to which various approaches including spectroscopic and electrochemical methods are applied, because they have allowed us to minimize effects of surface morphology and to obtain monolayer information [1–5]. Molecularly smoothed layers can be formed in much simpler ways; typical examples include Langmuir membranes formed on solution surfaces, L–B membranes, micelles, vesicles, etc. [6–8]. Molecules are loosely fixed on the surface in many cases, and continuous exchanges occur between molecules aligned along the surfaces and those dissolved in bulk.

Electrostatic effects dominate the distribution of ionic (and possibly polar) solutes in the vicinity of the charged surfaces, and influence reaction of these species. The electrostatic effects have been theoretically and experimentally well studied, and, it has been known that, in many instances, relatively simple models give good explanations to experi-

mental results. Additional effects are expected to come from a difference in solvent structures between the interfaces and bulk solution. Various approaches have revealed that solvent natures at interfaces are different from those in bulk; e.g., lower permittivity, highly oriented structures, and different solvation strength of solvents have been indicated [9–11]. Interfacial reactions may thus be different from reactions in bulk, but are often difficult to detect or distinguish from bulk reactions. Micelles are classical systems, but still provide attractive and versatile environments for interfacial studies. One of the major advantages of micelles over other interfaces is that a number of simple approaches are applicable because micellar systems are macroscopically homogeneous and transparent.

2-Hydroxy-azo compounds have been employed mainly for analytical purposes in combination with spectrophotometry, chromatography, solvent extraction, etc. [12–16]. Their high absorptivity and complexation capabilities have allowed the developments of a variety of analytical methods. In the present paper, our attention focuses on the reaction of a 2-hydroxy-azo compound at micellar surfaces. The introduction of a hydrocarbon chain to this class of compounds lowers the solubility in bulk water, and allows the polar active groups to be present at the solution/micelle interface

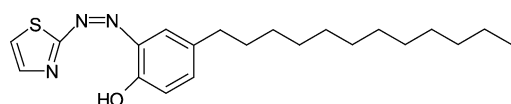
* Corresponding author.

E-mail address: tokada@chem.titech.ac.jp (T. Okada).

[17,18]. Because of the high absorptivity of the ligand and metal complexes, spectrophotometry is a simple and useful approach to investigate the reactions occurring at the interface. However, spectrophotometric studies possibly suffer from a serious disadvantage that the acid-base and complexation equilibria of 2-hydroxy-azo compounds often produce a number of colored species, and make the electronic spectra complicated. A factor and multivariate analysis is a powerful tool for separating the spectra of individual species and for extracting the information of the equilibria between these species [19–23], and should thus be suitable for studying the present system.

2. Experimental

2-Thiazolyl-azo-4-dodecylphenol (TADP),



TADP

was synthesized from 2-thiazolamine and 4-dodecyl-phenol by diazo-coupling. Oily product was dissolved in dichloromethane, and washed with aqueous sodium hydrogen carbonate several times. After evaporation of dichloromethane, the residue was dissolved in hexane, and products were extracted into methanol. Finally, TADP was purified by preparative silica gel chromatography with hexane–ethyl acetate (8:2) as the mobile phase; elemental analysis data (calculated values in parentheses), C = 67.61% (67.52%), H = 8.64% (8.36%), N = 10.95% (11.25%), S = 8.43% (8.58%). SDS of chemical grade was purified by recrystallization from methanol. Other reagents were of analytical grade. Solutions were prepared with water purified by a Milli-Q system. NaClO₄ was added to adjust the ionic strength of solutions.

Electronic spectra were recorded with a Shimadzu UV-visible spectrophotometer Model UV-2100, and processed with homemade programs written in Microsoft Visual Basic.

3. Principle of calculation

The principle of a factor analysis employed in this work is briefly described here; the details can be found in the literature [19].

A data matrix (**D**) is represented by the product of a spectral matrix (**R**) and a component matrix (**C**),

$$\mathbf{D} = \mathbf{RC}$$

An eigenvalue matrix (**E**) and an eigenvector matrix (**Q**) are extracted from a covariance matrix (**Z**),

$$\mathbf{Z} = {}^t\mathbf{DD} = {}^t\mathbf{QEQ}$$

After the number of pure components (n) is determined by referring to the eigenvalue matrix, new spectral (**R'**) and component matrices (**C'**) for n components are derived:

$$\mathbf{D} = \mathbf{R}'\mathbf{C}'$$

Assuming appropriate equilibria between n components, we can calculate their concentrations (**C***). The equilibrium constants and thus the most probable **C** and **R** are determined by selecting an optimum rotational matrix (**T**), which gives the minimum LSM_{conc} defined by

$$\text{LSM}_{\text{conc}} = \sqrt{\frac{\sum_i^n \sum_j^m ((C^*)_{i,j} - (TC)_{i,j})^2}{nm}}$$

where m refers to the numbers of samples.

4. Results and discussion

4.1. Electronic spectra and dissociation equilibria of TADP

TADP is highly insoluble in water, but soluble in SDS solutions, suggesting that TADP molecules be solubilized by partition into the micelles. The concentrations of SDS and TADP were kept constant (50 and 25 μM, respectively) throughout this work. Since the critical micellar concentration of SDS is 2.43 mM in, e.g., 0.05 M NaClO₄ solution, almost all of SDS molecules form micelles [24]. It has also been reported that the mean aggregation number of SDS is 60 [25]; one SDS micelle contains ca. 0.03 TADP molecules on an average under the present experimental condition. It can thus be reasonably assumed that the addition of TADP does not change the nature of the SDS micelles.

Figure 1 shows electronic spectra of TADP in SDS solutions of various pH. A broad absorption band is seen at $\lambda_{\text{max}} = \text{ca. } 450 \text{ nm}$ in acidic solutions. The λ_{max} shifts to 420 nm as pH increases, and a new absorption band appears at $\lambda_{\text{max}} = 520 \text{ nm}$ in basic solutions. The application of a factor analysis gave the following eigenvalues: 0.821, 0.173, 5.28×10^{-3} , 5.35×10^{-6} , ... This strongly indicates the contributions from three species to the entire spectra, which

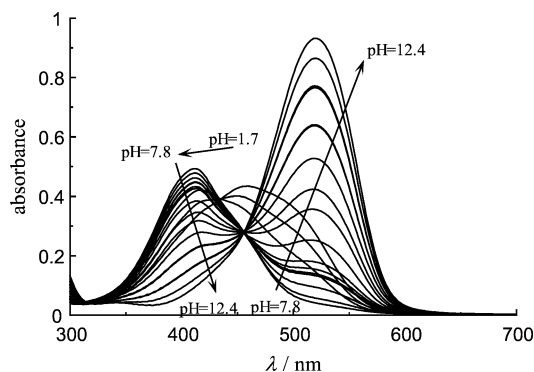


Fig. 1. pH dependence of electronic spectra of TADP. TADP = 25 μM, SDS = 0.05 M, and NaClO₄ = 0.05 M.

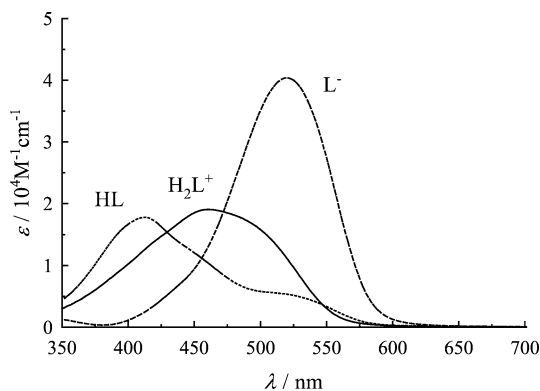
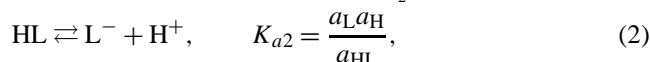
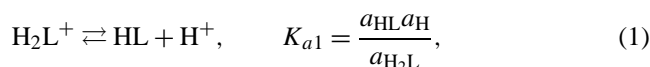


Fig. 2. Extracted molar spectra of TDAP species.

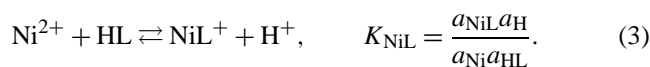
agree with the prediction based on the dissociation equilibria of TADP



where a refers to the activity of the compound represented by a subscript (valency was omitted for simplicity). The activity coefficients were calculated based on the extended Debye–Hückel law. The analysis of the spectra illustrated in Fig. 1 gave $\text{p}K_{a1} = 2.43$ and $\text{p}K_{a2} = 11.01$ with $\text{LSM}_{\text{conc}} = 1.7 \times 10^{-6}$ M. Figure 2 shows the extracted molar spectra of three chemical forms of TADP. The analytical procedure described above works very well for this relatively simple system.

4.2. Ni^{2+} complexation with TADP at the SDS micellar surface

Complexation of TADP with Ni^{2+} at the SDS micellar surface was investigated by a similar approach. Figure 3 shows the electronic spectra of TDAP– Ni^{2+} obtained with changing pH. The concentration of Ni^{2+} was kept 40 times as high as that of TDAP in order to avoid the multiple complexation, in which more than two TDAP molecules are involved. Although the entire spectral features are similar to those for TDAP itself, the detailed inspection implied that the spectra involve the contributions from TDAP– Ni^{2+} complexes. Factor and multivariate analyses are so useful to extract the spectral and equilibrium information of minor species that their application should facilitate to understand the chemistry of this system. The following complexation equilibrium was taken into account,



It should be noted that HL (not L^-) is mainly involved in complexation with Ni at moderate pH ranges judging from the dissociation constant of TDAP. However, the above equilibrium could not explain complicated spectral changes seen over the wavelength range 500–600 nm. Enlarged spectra are

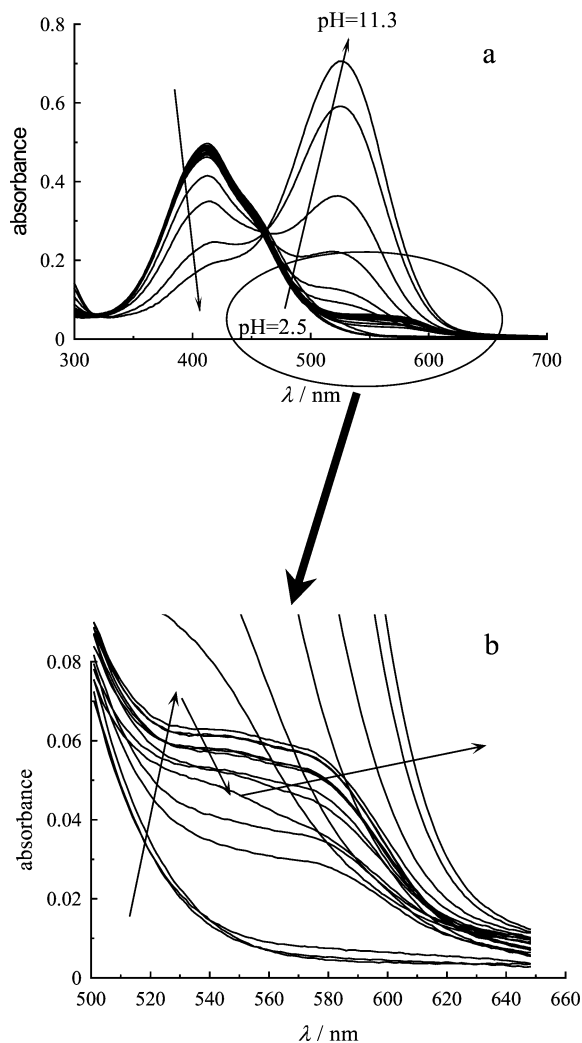
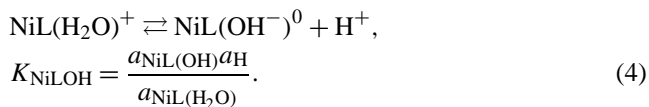


Fig. 3. Change in electronic spectra of Ni^{2+} –TDAP system. $\text{Ni}^{2+} = 1$ mM, TDAP = 25 μM , SDS = 0.05 M, and $\text{NaClO}_4 = 0.05$ M.

shown in Fig. 3b. In this wavelength range, the absorbance increases with increasing pH up to 8.7, decreases to pH 9.1, and then markedly increases due to the dominated contribution of L^- . This absorbance changes suggest that the involvement of another species formed around pH 9.

Since TDAP is a tridentate ligand, water molecules should coordinate Ni^{2+} in the 1:1 Ni^{2+} –TDAP complex. The deprotonation of water ligands will be facilitated by an electron withdrawing effect of the centered Ni^{2+} . Thus, it should be reasonable to introduce the following equilibrium:



The multivariate analysis was applied by assuming these equilibria (Eqs. (3) and (4)) and the hydroxo complex formation of Ni^{2+} in solution; hydroxo complex formation constants were taken from a reference, $\log \beta_1 = 3.08$ and $\log \beta_2 = 13$ [26]. Figure 4 shows the molar spectra of $\text{NiL}(\text{H}_2\text{O})^+$ and $\text{NiL}(\text{OH}^-)^0$ as well as those of HL and

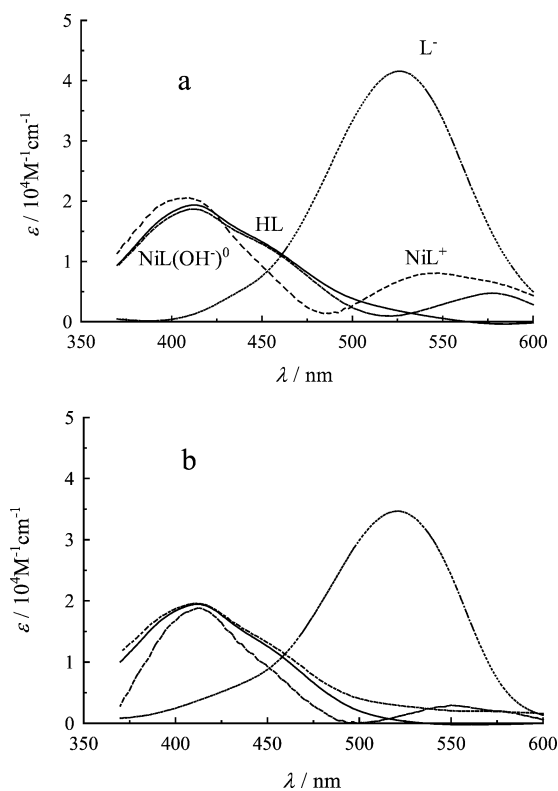


Fig. 4. Extracted molar spectra of TADP and its Ni^{2+} complex species. (a) 0.05 M NaClO_4 ; (b) 0.2 M NaClO_4 .

L^- extracted from a series of spectra, and compare the results obtained with different NaClO_4 concentrations. The two molar spectra of $\text{NiL}(\text{OH}^-)^0$ are slightly different in the wavelength range of 500–600 nm because of the strong adsorption of the L^- . However, almost the same molar spectra are derived from the spectra measured at different salt concentrations. In addition, the molar spectra of the ligand species agree with those obtained without Ni^{2+} , suggesting that the present calculation be successfully applied to the system under study. Since the concentrations of Ni^{2+} complexes are very low, the extracted molar spectra of Ni^{2+} complexes include ambiguities coming from their similar spectral features to ligand species. The equilibrium constants for Eqs. (3) and (4) were determined as $\log K_{\text{NiL}} = 5.43$ and $\log K_{\text{NiLOH}} = -9.03$ in 0.05 M NaClO_4 solution and $\log K_{\text{NiL}} = 4.55$ and $\log K_{\text{NiLOH}} = -8.45$ in 0.2 M NaClO_4 solution. The former set of values gives the changes in the concentrations of the species that are present in the TADP– Ni^{2+} system with pH as depicted in Fig. 5. $\text{NiL}(\text{H}_2\text{O})^+$ is formed at pH 6–10, while $\text{NiL}(\text{OH}^-)^0$ is formed at pH 8–11. The presence of these two complexes causes the spectral changes over this alkaline pH range.

4.3. Electrostatic equilibrium shift at the surface of SDS micelles

Various equilibrium shifts due to electrostatic effects have been studied to evaluate electrostatic potential [27–29].

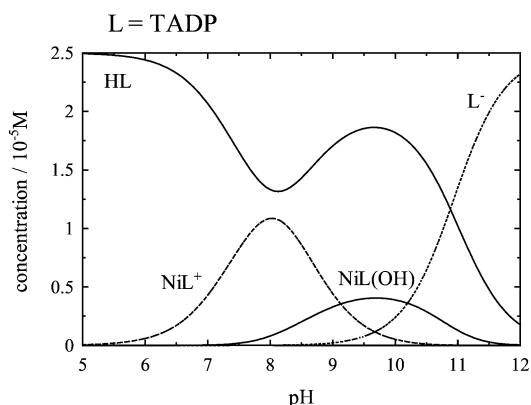


Fig. 5. Distribution of TADP and its complexes with Ni^{2+} in 0.05 M SDS and 0.05 M NaClO_4 solution.

When a molecular probe is present on the micellar surface, unambiguous evaluation of the surface potential is feasible. TADP is a water-insoluble compound, and entirely entrapped by the SDS micelles. Although there is still ambiguity in regard to the exact location of TADP molecules, it is reasonable to assume that a relatively hydrophilic thiazoryl-azo group exists in the palisade portion of the micelle, and thus the equilibria of TADP undergo electrostatic effects. In order to evaluate electrostatic effects on the acid dissociation of TADP, the acid dissociation of its water-soluble analogue, thiazoryl-azo-cresol (TAC), was investigated in a similar way. Its dissociation constant was determined as $\text{p}K_{a2} = 7.97$, which is obviously larger than that of TADP at the micellar surface. An effect of the alkyl group on the dissociation of phenolic hydroxyl groups is so marginal that this difference is not caused by substituting the dodecyl group in TADP by a methyl group. It has been pointed out that there are two effects in the equilibrium shifts occurring at the micellar surfaces, i.e., electrostatic and environmental effects [27,28]; the precise evaluation of the latter one is generally difficult. Assuming that the equilibrium shift in the present case is caused solely by the negative surface potential of the SDS micelles, the surface potential is given by the following equation:

$$\psi = -2.3 \frac{RT}{F} (\text{p}K_{a\text{TADP}} - \text{p}K_{a\text{TAC}}). \quad (5)$$

This equation is derived by assuming that hydrogen ions are condensed in the vicinity of the micellar surface by the negative surface potential of the SDS micelles, and in turn pH should be lowered in comparison with the corresponding bulk value. The potential of the SDS micelle surface was determined as -180 mV. It has been reported that the surface potential of the SDS micelle is -100 mV in 0.05 M Na^+ solution [28], which is less negative than that determined in the present work. The micellar surface potential is discussed below in more details on the basis of the electrostatic calculations.

As noted above, the equilibrium constants depend on the electrolyte concentration. Effects of electrolyte concentration on the equilibrium constants can be discussed on the

basis of micellar surface potential,

$$\Delta\psi = -2.3 \frac{RT}{F} (\log K^1 - \log K^2), \quad (6)$$

where K^1 and K^2 denote equilibrium constants determined for different electrolyte concentrations. The differences in the SDS micellar surface potential between in 0.05 M and 0.1 M NaClO₄ and between in 0.05 M and 0.2 M NaClO₄ were determined as 30 mV and 58 mV based on the equilibrium shifts of K_{a2} , respectively. As discussed above, the surface potential of the SDS micelle was estimated -180 mV in 0.05 M NaClO₄ with TAC as a water-soluble reference. Thus, the surface potential becomes less negative with increasing electrolyte concentration, as -150 mV in 0.1 M NaClO₄ and -122 mV in 0.2 M NaClO₄ solution. The equilibrium shifts of K_{NiL} and K_{NiLOH} also gave the difference between 0.05 M and 0.2 M NaClO₄ solutions as 52 and 34 mV.

The potential differences were estimated based on Poisson–Boltzmann theory to test the validity of the above values. SDS micelles can be regarded as a sphere, and thus the solution of Poisson–Boltzmann equation for the spherical geometry should give the surface potential of the micelle. When a spherical charged body is present in 1:1 electrolytes, the following equation can be used for estimating the surface potential (ψ_0) [30],

$$\sigma_{\text{eff}} = \frac{2\varepsilon_0\varepsilon RT}{F} \sinh\left(\frac{F\psi_0}{2RT}\right) \times \left[1 + \frac{2}{\kappa a \cosh^2\left(\frac{F\psi_0}{4RT}\right)} + \frac{8 \ln\{\cosh\left(\frac{F\psi_0}{4RT}\right)\}}{(\kappa a)^2 \sinh^2\left(\frac{F\psi_0}{2RT}\right)} \right]^{1/2}, \quad (7)$$

where a is the radius of a charged sphere, σ_{eff} is the effective surface charge density, κ is the Debye shielding parameter, and R , T , ε , ε_0 , and F have usual meanings. For the SDS micelles, a and the aggregation number have been reported to be 1.67 nm [31] and 60 [25], respectively. The charge density, σ , is thus estimated to be 0.32 C m^{-2} if all the sulfate groups are dissociated. It is well known that the dissociation of counterions (α) from micelles is almost constant; for SDS, several values have been reported, i.e., $\alpha = 0.27$ – 0.35 , meaning that 65–73% of the total sulfate groups on the SDS micellar surface bind Na⁺ [32,33]. The effective surface charges are substantially reduced, and, in turn, the surface potential is also lowered than that calculated from σ . The ion-association constant of Na⁺ with the sulfate groups on the micellar surface, K_m^{Na} , was introduced to take the reduction of effective charges into consideration. Thus, the effective surface charge density of the micelle is given by

$$\sigma_{\text{eff}} = \sigma \frac{1}{1 + [\text{Na}^+] K_m^{\text{Na}} \exp\left(-\frac{F\psi_0}{RT}\right)}.$$

The exponential term represents the condensation of Na⁺ due to the negative potential in the vicinity of the SDS micellar surface. When K_m^{Na} is set to 1 M^{-1} , α ranges from 0.34 to

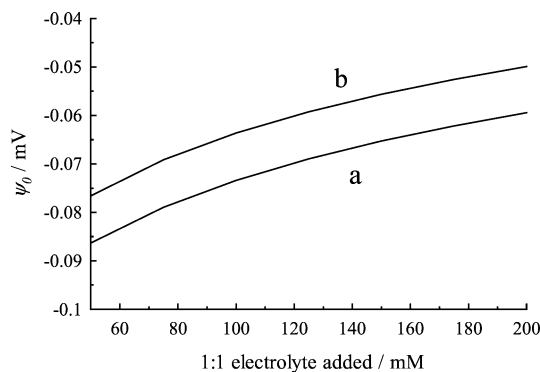


Fig. 6. Calculated surface potential of the SDS micelle. (a) $K_m^{\text{Na}} = 1 \text{ M}^{-1}$; (b) $K_m^{\text{Na}} = 2 \text{ M}^{-1}$. Details are given in the text.

0.36 when no electrolytes are added, slightly depending on the SDS concentration. Similarly, when K_m^{Na} is set to 2 M^{-1} , α ranges from 0.27 to 0.28. These values agree with reported α values. The surface potential was thus calculated by setting $K_m^{\text{Na}} = 1$ and 2 M^{-1} . Figure 6 shows the dependence of the surface potential on the 1:1 electrolyte concentration. Regardless of assumed K_m^{Na} values, differences in the surface potential between at $[\text{Na}^{2+}] = 0.05 \text{ M}$ and 0.2 M are ca. 30 mV, which is lower than the values estimated from the equilibrium shift as stated above. There are at least two possible explanations for this discrepancy; (1) the micellar surface environments (for the reason other than electrostatic) make a particular structure or species thermodynamically preferable and (2) the micellar surface reaction occurs at the different distance from the micellar surface, and therefore undergoes different electrostatic effects. The ambiguities in the location of a probe molecule may imply the limitation of the molecular probe to evaluate electrostatic potential. However, the above calculation cannot explain larger potential differences even though any distance parameters are substituted into the equations. Aqueous environments around the micelle, which is different from bulk solution, facilitate the formation of unusual complex such as $[\text{TDAP}(\text{OH}^-)\text{Ni}]^0$. It is reasonable to consider that this specific reaction field causes the deviation from the prediction of the simple electrostatic theory.

References

- [1] D.A. Smith, M.L. Wallwork, J. Zhang, J. Kirkham, C. Robinson, A. Marsh, M. Wong, *J. Phys. Chem. B* 104 (2000) 8862.
- [2] P.K. Singh, J.J. Adler, Y.I. Rabinovich, B.M. Moudgil, *Langmuir* 17 (2001) 468.
- [3] J. Zhang, J. Kirkham, C. Robinson, M.L. Mallwork, D.A. Smith, A. Marsh, M. Wong, *Anal. Chem.* 72 (2000) 1973.
- [4] F.P. Zamborini, J.F. Hicks, R.W. Murray, *J. Am. Chem. Soc.* 122 (2000) 4514.
- [5] J.J. Gooding, P. Erokhin, D. Losic, W. Yang, V. Policarpio, J. Liu, F.M. Ho, M. Situmorang, D.B. Hibbert, J.G. Shapter, *Anal. Sci.* 17 (2001) 3.
- [6] K. Iso, T. Okada, *Langmuir* 16 (2000) 9199.
- [7] J.B. Peng, G.T. Barnes, I.R. Gentle, *Adv. Colloid Interface Sci.* 91 (2001) 163.
- [8] M.B. Forstner, J. Käs, D. Martin, *Langmuir* 17 (2001) 567.

- [9] I. Benjamin, *Chem. Rev.* 96 (1996) 1449.
- [10] D. Michael, I. Benjamin, *J. Chem. Phys.* 114 (2001) 2817.
- [11] J.E. Pemberton, S.L. Joa, A. Shen, K.J. Woelfel, *J. Chem. Soc. Faraday Trans.* 92 (1996) 3683.
- [12] J. Ruzicka, A. Arndal, *Anal. Chim. Acta* 216 (1989) 243.
- [13] T. Naito, Y. Tsuiki, H. Yamada, *Anal. Sci.* 17 (2001) 291.
- [14] A. Ohashi, H. Watarai, *Anal. Sci.* 17 (2001) 1313.
- [15] H. Hoshino, T. Yotsuyanagi, *Talanta* 31 (1984) 525.
- [16] L. Sommer, V. Kuban, L. Langove, *Fresenius J. Anal. Chem.* 310 (1982) 51.
- [17] D. Fornasiero, F. Grieser, W.H. Sawyer, *J. Phys. Chem.* 92 (1988) 2301.
- [18] J.K. McCulloch, D. Fornasiero, J.M. Perera, B.S. Murray, G.W. Stevens, F. Grieser, *J. Colloid Interface Sci.* 157 (1993) 180.
- [19] T. Ozeki, H. Kihara, *Anal. Chem.* 60 (1988) 2055.
- [20] M. Kubista, R. Sjöback, B. Albinsson, *Anal. Chem.* 65 (1993) 994.
- [21] V. Tomišić, V. Simeon, *Phys. Chem. Chem. Phys.* 1 (1999) 299.
- [22] J. Ghasemi, A. Niazi, M. Kubista, A. Elbergali, *Anal. Chim. Acta* 455 (2002) 335.
- [23] R. Sjöback, J. Nygren, M. Kubista, *Spectrochim. Acta A* 51 (1995) L7.
- [24] D.E. Dunstan, L.R. White, *J. Colloid Interface Sci.* 134 (1990) 147.
- [25] F. Grieser, C.J. Drummond, *J. Phys. Chem.* 92 (1988) 5580, and references therein.
- [26] Kagaku Binran [Chemical Index], Maruzen, Tokyo, 1993.
- [27] O.A. El Seoud, *Adv. Colloid Interface Sci.* 30 (1989) 1.
- [28] M.S. Fernández, P. Fromherz, *J. Phys. Chem.* 81 (1977) 1755.
- [29] R. Sjöback, J. Nygren, M. Kubista, *Biopolymers* 46 (1998) 445.
- [30] H. Ohshima, T.W. Healy, L.R. White, *J. Colloid Interface Sci.* 90 (1982) 17.
- [31] J.B. Hayter, J. Penfold, *Colloid Polym. Sci.* 261 (1983) 1022.
- [32] G. Charbit, F. Dorion, R. Gaboriaud, *J. Colloid Interface Sci.* 106 (1985) 265.
- [33] B.L. Bales, *J. Phys. Chem. B* 105 (2001) 6798.